**NURETH14-109** 

# APPLICATION OF THE BALLOONING ANALYSIS CODE MATARE ON A GENERIC PWR FUEL ASSEMBLY

# L. Ammirabile<sup>1</sup>, S. P. Walker<sup>2</sup>

<sup>1</sup> European Commission, JRC, Institute for Energy, Petten, The Netherlands <sup>2</sup> Imperial College London, London, United Kingdom

#### **Abstract**

The MATARE (MAbel-TAlink-RElap) code is a new multi-pin deformation analysis code created through the dynamic coupling between the thermal-hydraulic code RELAP5 and multiple instances of the single-pin thermal-mechanics code MABEL. A multi-pin representation of different zones of a typical PWR fuel assembly under post-LOCA reflooding conditions was analysed including some of the most relevant features that characterise a typical nuclear reactor fuel assembly and evaluate their effect on the behaviour of the fuel rods under conditions leading to clad ballooning. The code was able to simulate the deformation of wide regions of a fuel assembly under reflood conditions and has shown how differences in pin pressure and the presence of rod with burnable poisons and control rod guide thimbles also contribute to a substantial incoherent ballooning in agreement with the experimental data.

#### Introduction

Clad ballooning is basically a creep phenomenon occurring under degraded cooling conditions and it is driven by the internal pin pressure. Under Design Basis Conditions (DBC), clad ballooning might occur in the reflooding phase of a Large Break Loss-Of-Coolant Accident (LB-LOCA) [1]. It was nevertheless observed at the Three Mile Island (TMI) accident and it is believed to have occurred during the first core degradation phases of the recent Fukushima accident.

Such ballooning will cause the cladding to approach the cladding of neighbouring pins, which themselves may also be ballooning. The flow area available for cooling vapour, and eventually liquid water coolant, will be reduced. If large numbers of adjacent pins all balloon over similar axial locations, there could be sizeable regions of the core to which the re-flood water gains little or no access. Decay heating will continue, and widespread fuel melting and clad failure becomes a possibility.

Experiments dedicated to clad ballooning under post-LOCA reflooding conditions have shown that axial deformation profiles within fuel assemblies vary between rods, and the locations of the positions of peak strain may be sufficiently different to reduce coolant channel blockage considerably.

Different reasons may explain the experimental results and justify why blockages due to swelling might not be coherent. In essence this is because pins are not identical, and/or they are not exposed to identical conditions. Both systematic and stochastic effects contribute to distinguish fuel pins

within the assembly. Systematic differences; that is, differences which can be predicted, include, for example flux variations across the core or pin to pin power variations due to proximity to control rods and control rod guide tubes or the addition of burnable poisons in the pellets. Stochastic differences embrace, for example, random manufacturing differences in pellet dimensions and compositions, geometrical non-uniformities. Fill gas pressurisation is similarly subject to some random variation. If one rod deforms more rapidly than its neighbours, the coolant flow around it is reduced and the diverted flow enters neighbouring sub-channels, cooling surrounding rods more. The temperature of surrounding rods may also be important if contact is achieved. A cooler neighbouring rod would reduce the rate of deformation, resulting in axially extended balloons. A hotter neighbouring rod destabilises the deformation, leading to early failure. The main aim of this study was to include in the coupled thermal-hydraulic and structural mechanics model MATARE some of the most relevant features that characterise a typical nuclear reactor fuel assembly and analyse their effect on the behaviour of the fuel rods under conditions leading to clad ballooning. The MATARE (MAbel-TAlink-RElap) code has the unique feature of being the first ever mechanistically-coupled thermal hydraulic-structural mechanics analysis tool able to study a significant number of fuel pins in a coupled fashion.

A multi-pin representation of three different zones of a typical PWR fuel assembly was analysed with the MATARE code in the reflooding conditions following a Large Break LOCA. The validation of MATARE against the MT3 experiment [2], [3] was used as a convenient point of departure, and all the other characteristics, including the geometry, the thermal-hydraulic conditions, the eccentricity values of direction and magnitude, were identical to the ones used for the MT-3 validation. In this way, a direct comparison with the MT-3 experimental results could be performed and the differences identified.

The features analysed included different fuel burn-ups, the presence of burnable poisons (Gadolinium oxide), and the existence of the control rod guide thimbles. The incorporation of such characteristics increases the level of differences between the rods, leading generally to a more incoherent ballooning.

# 1. PWR fuel assembly

In most of PWR designs, each assembly consists of a 17 x 17 array in square lattice configuration (Figure 1). Each fuel rod contains a stack of fuel pellets enclosed in a Zircaloy cladding tube seal-welded with end plugs. The fuel pellets consist of sintered uranium dioxide (UO<sub>2</sub>) enriched in the fissile material U<sub>235</sub> to between 3 and 4%. Uranium dioxide features an outstanding fission product retention capability and is highly insensitive to corrosive attack by the coolant in the event of cladding tube defects. To control the excess in reactivity and provide a higher fuel Burnup, burnable poisons are added into the fuel matrix. Burnable poisons are materials that have a high neutron absorption cross-section that are converted into materials of relatively low absorption cross section as the result of neutron absorption. Due to the burnup of the poison material, the negative reactivity of the burnable poison decreases over core life. Fixed burnable poisons are generally used in the form of compounds of gadolinium and introduced as additives to the fuel. Since they can usually be distributed more uniformly than control rods, these poisons are less disruptive to the core power distribution and avoid over-moderation of high boron loading. Fuel pellets may contain 3 to 9% neutron-absorbing gadolinium oxide (Gd<sub>2</sub>O<sub>3</sub>).

The fuel rods are internally pressurised with helium to enhance thermal conduction between the fuel and the cladding tube. The internal pressure increases during the residence time of fuel in the core as gaseous fission products add up in the cladding together with stochastic variation in the rod free gas plenum volume. Of the 289 spaces available in an assembly, 264 are occupied by fuel rods; the remaining spaces contain guide tubes (thimbles) for control rods with a central tube available for instrumentation (as movable neutron flux detectors). About one third of the assemblies in the core actually include control rod. In the other assemblies the guide tubes are partially blocked. Grid spacers provide a degree of lateral support, and hold the fuel rods in such a way that axial expansion is unrestrained and channel cross sections are equal.

In the analysis a PWR fuel assembly with a mean irradiation of 16 GWd/tU containing rods with burnable poisons was considered in reflooding conditions following a Large Break Loss-Of-Coolant Accident. The three PWR sub-assembly regions analysed are indicated in Figure 1. The design parameters of the fuel assembly are set to be the same as in the MT-3 experiment, and are shown in Table 1.

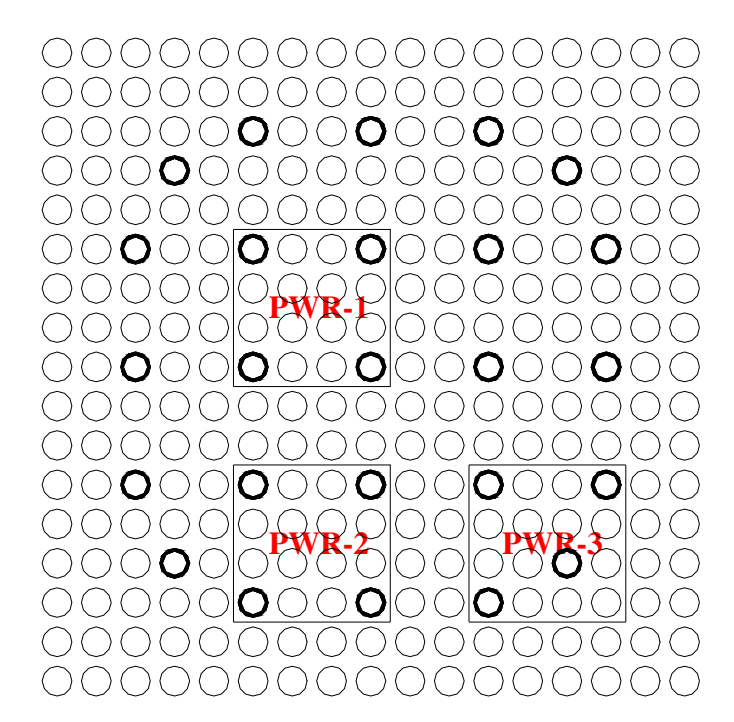


Figure 1 PWR Sub-assembly regions analysed

Cladding Outside Dimension	9.63mm	
Cladding Inside Dimension	8.41mm	
Fuel Pellet Diameter	8.26mm	
Fuel Pellet Length	9.53mm	
Active Length	3657.6mm	
Rod-Rod Pitch	12.75mm	

Table 1 Fuel assembly Design Parameters

# 2. The MATARE Model of the three PWR assembly Regions

MATARE is a computational tool derived from the coupling of three pre-existing codes: the NRC system code RELAP5 [4], the fuel rod modelling code MABEL [5] and the dynamic coupling code TALINK [6].

Fuller details of MATARE (internal gas pressure calculation, cladding burst criteria, high-temperature cladding creep computation) can be found in [5] and in the work of Ammirabile [3], [7], [8] but in essence the MATARE model is as follows.

The thermal-hydraulic code RELAP5 models the sub-channels of a bundle of rods by means of hydraulic (pipes) and heat structure components connected through crossflow junctions introduced to permit lateral movement of coolant between sub channels. Each of the rods being analysed is represented by an instance of the MABEL fuel rod modelling code. The thermal-hydraulic boundary conditions for the MABEL code are proved by RELAP5, with the data being passed via TALINK. MABEL computes the cladding size, and this in turn is passed back to RELAP5 to modify the geometry of the subchannels. In addition to the MABEL to RELAP5 data transfer, instances of MABEL communicate to each other to model the iteration of adjacent rods. The specific model for the sub-assembly regions are described hereafter.

## 2.1 RELAP5 Model

The RELAP5 model for the three PWR sub-assembly regions is shown in Figure 2. This consists axially of three sections: the lower plenum, the core sub-channels and the upper plenum. The lower and upper plena are simulated with branch components and are connected through multi-junction components respectively to the bottom and the top of each core sub-channel.

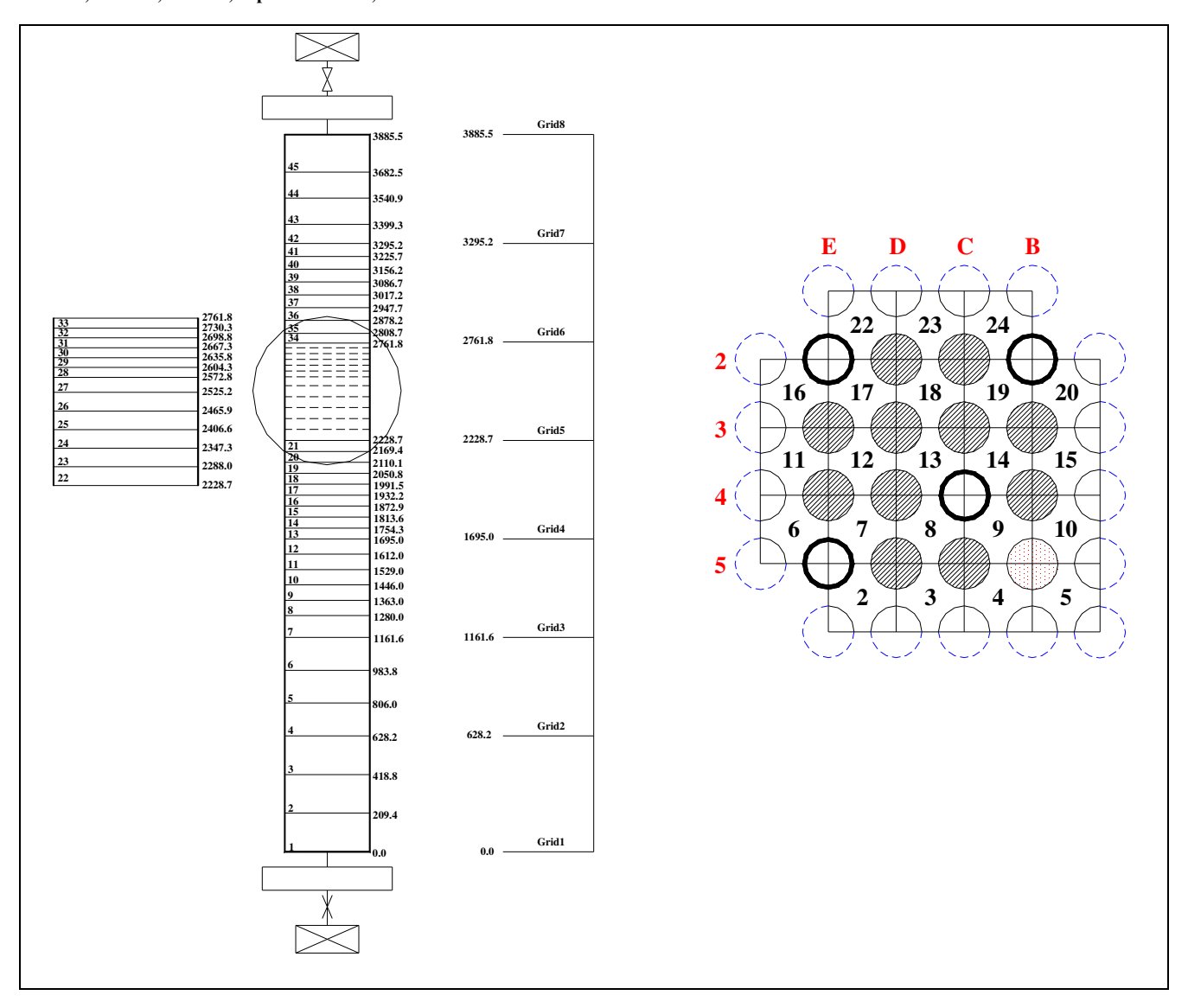


Figure 2 Relap5 model (Chn. 5 in PWR-3 model)

The core model consists of 21 (22 for PWR-3 region) hydraulic (pipe) components to simulate each inner sub-channel. All the hydraulic components are interconnected as appropriate through cross-flow junctions (for example, channel 17 is connected to channels 12, 16, 18 and 22. The use of cross-flow junctions however only approximates to a three-dimensional system since the momentum cross product lacks of the transverse convection component of axial momentum that is assumed zero. This is not generally true in a rod bundle geometry, where the transverse flow usually retains its axial momentum, but can be tolerated if transverse momentum fluxes are negligible.

A time-dependent volume and related trip valve controls the rig pressure, while a time-dependent junction and related time-dependent volume provide to the same flow rate of water as that injected during reflood.

#### 2.2 MABEL model

For each region, twelve pressurised rods are individually analysed using twelve different simultaneous Mabel instances. The differences in pin power and internal pressure, deriving from the different peak factors could be fully modelled. The fuel rod design characteristics were as in Table 1, and identical for each rod. No assumption of possible random manufacturing differences has therefore been included in the analysis.

To analyse the sharply-peaked strain distributions and the response of partial cladding contact after rod trapping the number of cladding azimuthal nodes and heat transfer azimuthal nodes was set to the maximum (16).

The constraint induced by the swelling of the neighbour rods was simulated assuming that their deformation (and clad temperature) reflects that of the rods according to the scheme shown in Figure 3.

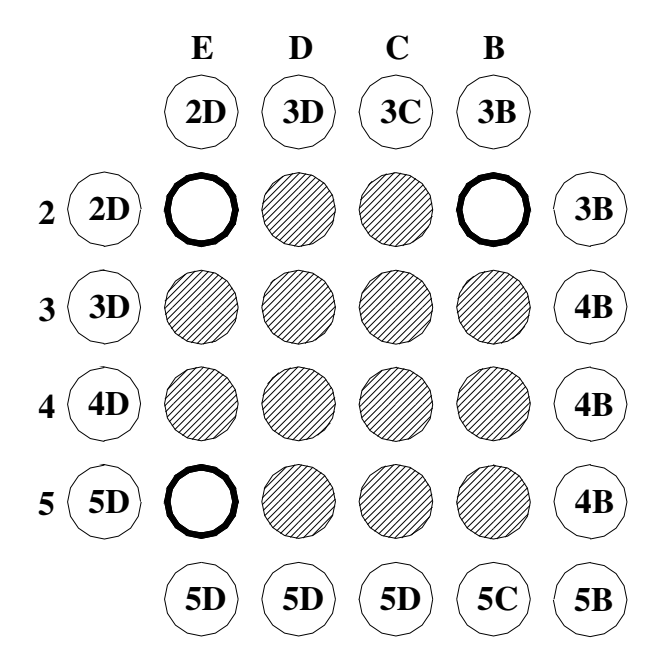


Figure 3 Surrounding rods (5B in the PWR-3 Case)

The "restrained" mechanical restraint model was adopted for all the twelve Mabel instances. This model allows the rod to flatten as soon as it comes in contact with two opposite outer rods. Creep constants are the same as used in the MT-3 experiment and are based on CEGB recommendations [9]. A good agreement with experimental results over a range of circumferential extensions and azimuthal temperature differences was shown using this criterion in previous calculations [10].

The MATARE grid model based on the Yao, Hochreiter and Leech correlation [11] was used to simulate spacer grids along the assembly.

## 2.3 Initial and boundary conditions

The initial and boundary conditions adopted in the MATARE model were mainly extracted from the MT-3 experiment.

The upper plenum pressure was kept constant at 0.28 MPa while the inlet water temperature was set at the constant value of 311K.

To achieve a long-duration thermal transient at almost constant temperature, in the ductile temperature range of the upper zone of the  $\alpha$ -phase it was necessary to have an initial period of predetermined reflood rates. The flow velocity time-dependence, used in the simulation, is shown in Figure 4.

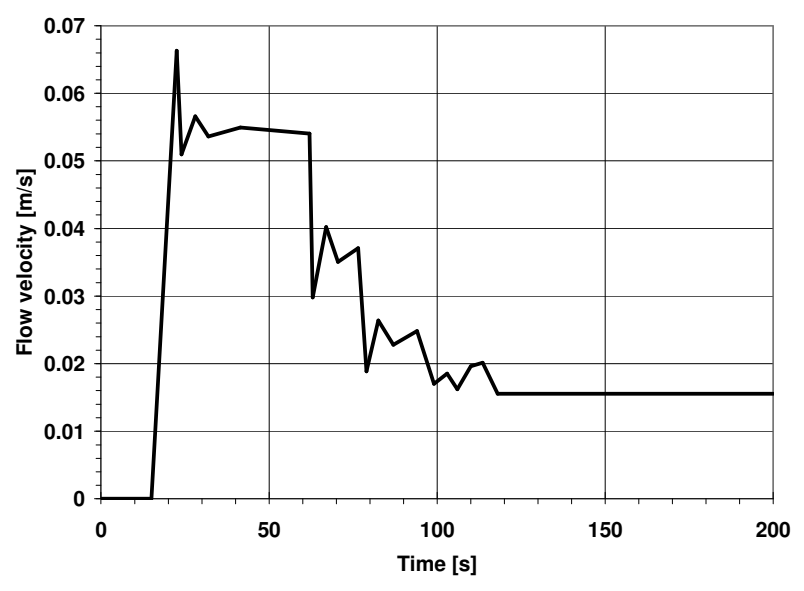


Figure 4 Reflood water flow velocity

The internal rod pressure and rod power are affected by the rod peak factor. A fuel assembly with a mean irradiation of 16 GWd/tU containing rods with burnable poisons was considered (Figure 5).

	1.049	1.053		1.067	<u>0.757</u>		1.025	0.992
1.049	1.037	1.046	1.059	1.045	1.056	1.050	1.009	0.990
1.053	1.046	0.744	1.067	1.050	0.743	1.051	1.009	0.988
	1.059	1.067		1.061	1.063		1.021	0.989
1.067	1.045	1.050	1.061	1.048	1.059	1.045	1.001	0.983
<u>0.757</u>	1.056	0.743	1.063	1.059		1.036	0.989	0.973
	1.050	1.051		1.045	1.036	<u>0.715</u>	0.981	0.967
1.025	1.009	1.009	1.021	1.001	0.989	0.981	0.964	0.961
0.992	0.990	0.988	0.989	0.983	0.973	0.967	0.961	0.964

Figure 5 Peaking factors of quarter PWR fuel assembly with 16GWd/tU mean irradiation (Gd-poisoned rods are in green).

For the conditions of interest a reasonable way of representing the pin internal pressure is:

$$P_{\text{int}} = 5.5 + 3.6 \text{ Fdh (MPa)}$$
  
For UO<sub>2</sub> pin: (1)

$$P_{int} = 6.5 + 2.9 \text{ Fdh. (MPa)}$$
 (2)

The differences in pin power and internal gas pressure due to the different peak factors for each case are shown in Figure 6.

The eccentricity, chosen for each rod, was taken from the MT-3 validation study [3] and is shown in Table 2

Rod	Value	Angle (rad)	Rod	Value	Angle (rad)
2C	1.0	0.7854	4B	0.95	2.0944
2D	0.35	2.9670	4C (5B)	0.75	2.3562
3B	0.25	3.4906	4D	0.65	5.2360
3C	0.5	4.8849	4E	0.45	4.3633
3D	0.35	5.4978	5C	0.05	0.7854
3E	0.35	1.5708	5D	0.25	1.7453

Table 2 Eccentricity values (5B in PWR-3 Case)

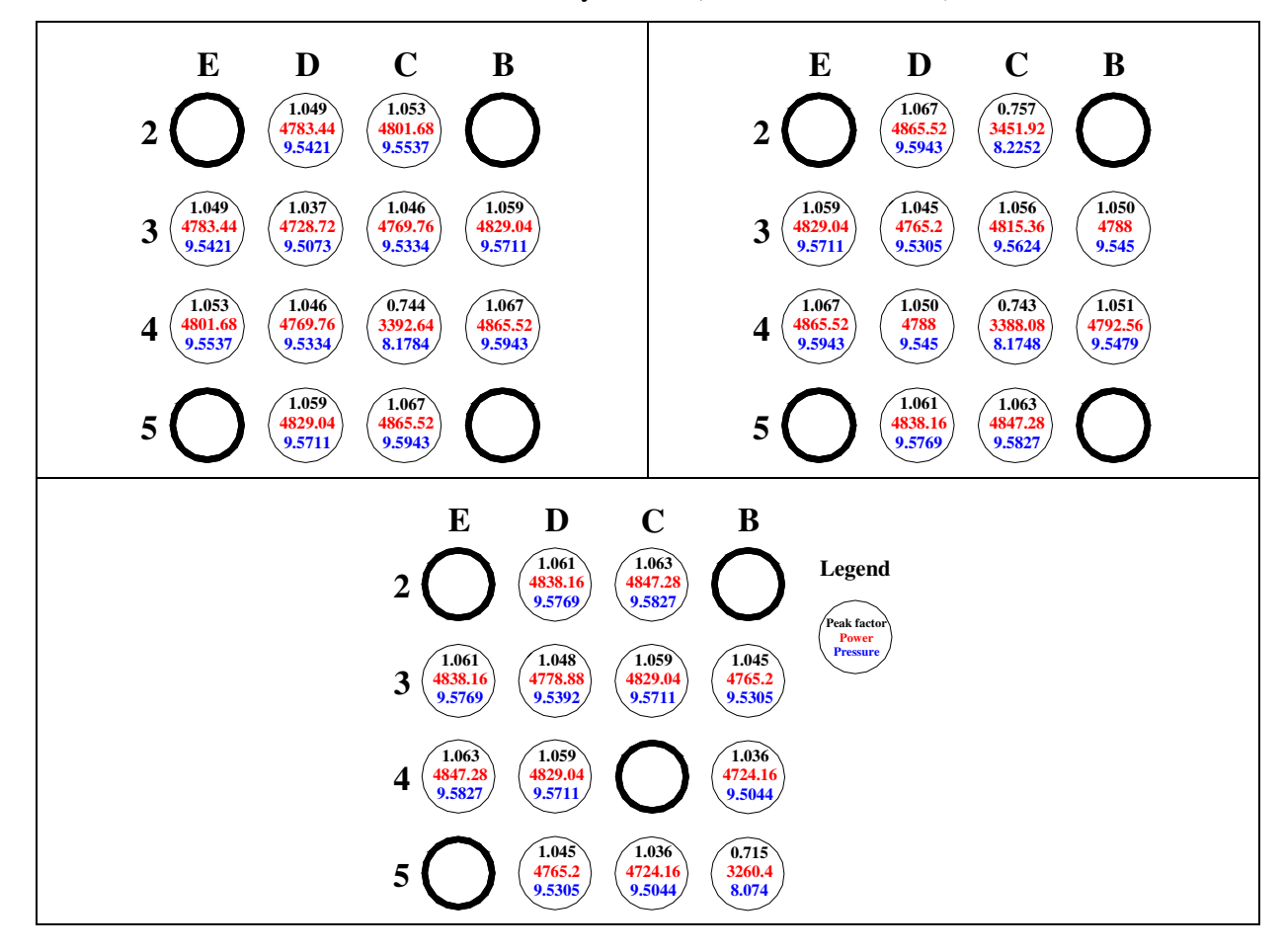


Figure 6 Fuel rod peak factor, power and initial gas pressure

## 3. Results

## 3.1 Clad surface temperatures

In Figure 7 are shown the cladding temperatures throughout the reflooding phase in the three sub-assembly regions as computed with MATARE.

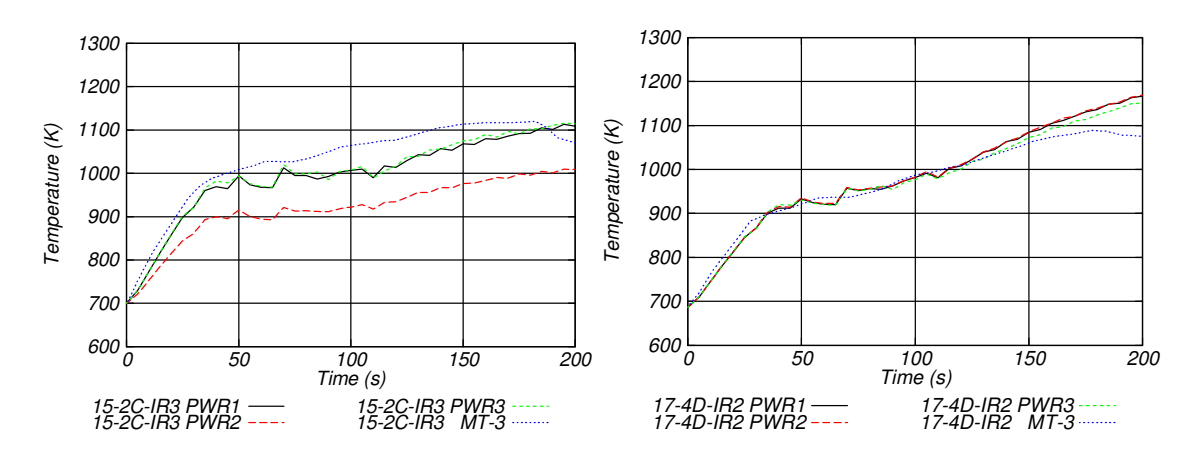


Figure 7 Rod Surface Temperatures at Level 15 and Level 17

Values of two different rods (2C and 4D) at two axial locations, level 15 and level 17, are shown, for each of three regions. The MT-3 experimental temperatures at the same locations are also given.

The temperature trends are similar for all three regions at all locations with the exception of rod 2C in PWR-2 Case. Here rod 2C is poisoned with Gadolium, which causes the rod to have a small peak factor and hence a low decay power. The rise in cladding temperature during the uncooled heat up phase was therefore lower compared to the other rods with a higher decay power.

The temperature histories similar to the MT-3 temperature trends show that the rods in all three regions undergo a prolonged residence in the ductile temperature range of the upper zone of the  $\alpha$ -phase as in the MT-3 experiment. Such a transient is considered to be conducive to the severe development of long balloons with large diametrical strains.

#### 3.2 Azimuthal and axial strains

The calculated axial strain profiles in the three analysed regions are presented in Figure 8.

Three peaks in ballooning, also observed in the MT-3 experiment, are clearly visible in the rods without burnable poisons. The grids cause downstream an enhanced mixing of steam and water improving the heat transfer. This effect, accurately reproduced by the MATARE grid model, decays exponentially along the rod and results in carrot-shaped balloons where the region of significant growth is restricted to the top end of each grid span.

The axial strain profile of the rods with burnable poisons shows a small peak upstream the fourth grid, followed by a plateau upstream the fifth grid and a bigger peak downstream the fifth grid. Rods with burnable poisons undergo little deformation causing a small sub-channel blockage compared to the adjacent rods.

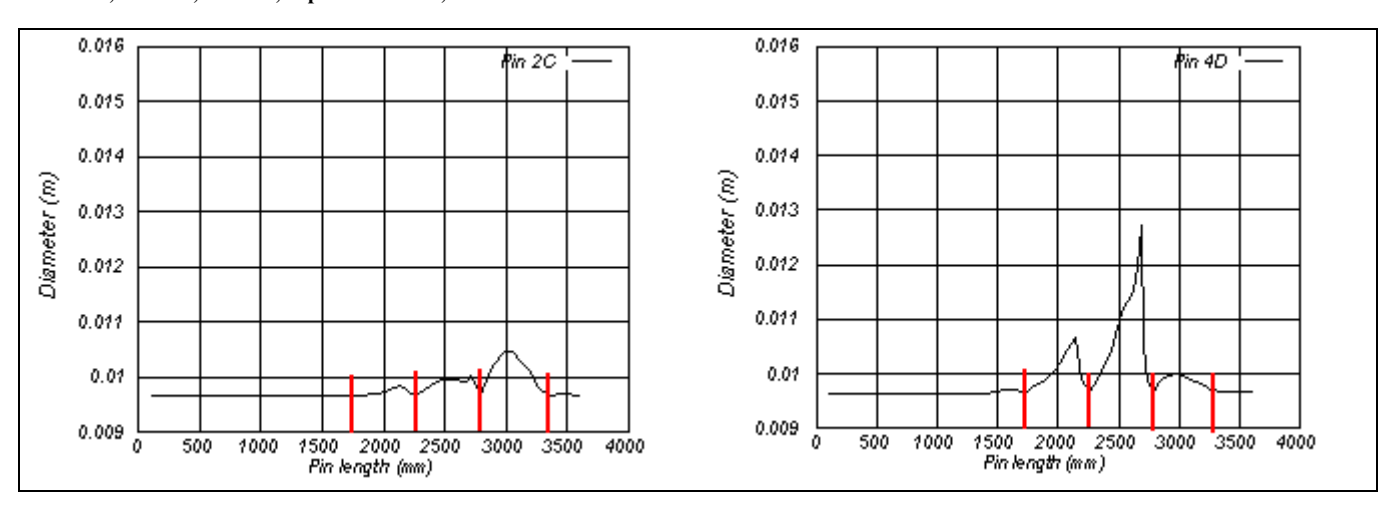


Figure 8 Axial strain profiles rod 2C-PWR2 and rod 4D-PWR3 (in red the grids positions)

The flow diversion towards the sub-channels around the poisoned rod leads to better cooling conditions generating the plateau observed upstream the fifth grid. The only modest peak, is downstream the fifth grid, where the cladding temperature is high enough to cause deformation. The lateral displacement and azimuthal shape of the pressurised rods in the three regions at rupture node 31 (2670 mm) is presented in Figure 9.

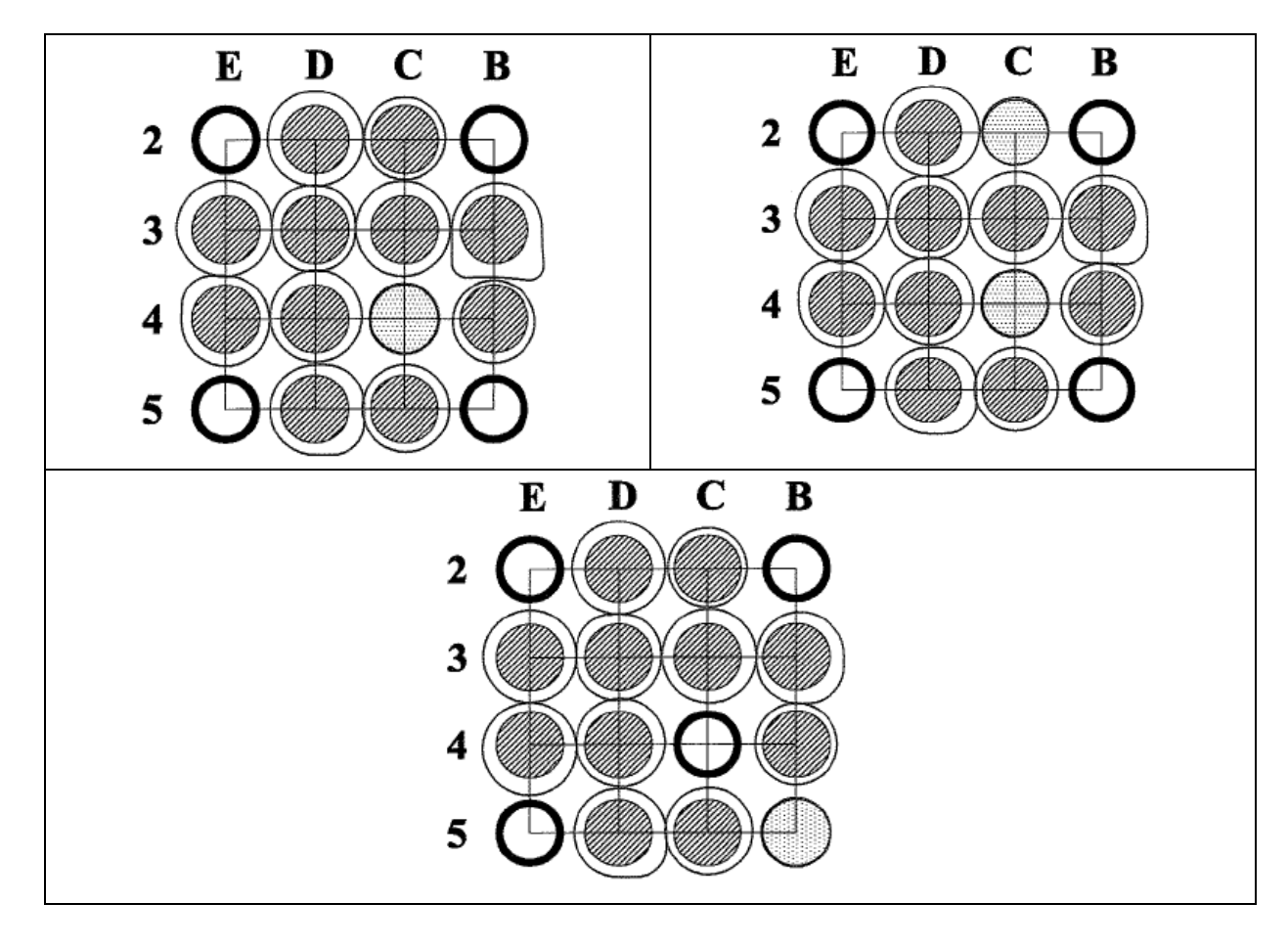


Figure 9 Azimuthal Rod shapes

No relevant outward movement of the ballooning rods is observed in the three cases. This is likely to occur in a fuel assembly, where the simultaneous deformation of several rows of rods leaves little room for the rods themselves to move apart. Only the nil or very low strain of the guide thimbles and the rods with burnable poisons provide some space for the adjacent rods to move apart.

The sub-channel blockage around guide thimbles and poisoned rods is low. The flow diversion towards these sub-channels, providing high azimuthal temperature gradients in the surrounding rods, causes them to fail before serious blockage can take place.

# 3.3 Pin pressure

Pressures in all rods are predicted to behave more or less identically during the transient until the failure time. Different initial rod pressures were given according to the different peak factors (from about 8.0 to 9.6 MPa). The rods experience a similar rise in pressure during the uncooled heat-up period to a maximum value, and then fall slowly with almost the same slope until failure. The rods with burnable poisons show a less steep descending slope.

In Figure 10 are shown the pressure transients of rod 2C in the three sub-assembly regions together with the experimental pressure history in the MT-3 experiment. The time trends are similar with no evidence of plenum quench during the transient.

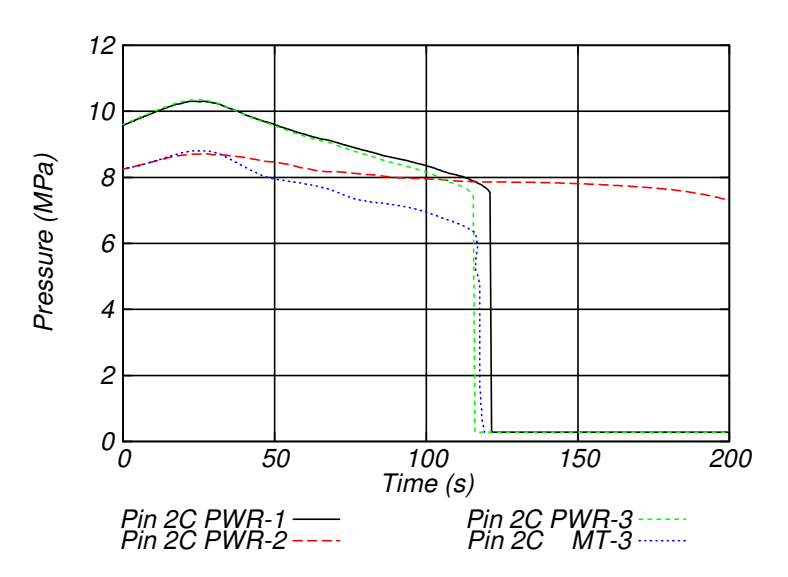


Figure 10 PWR sub-assembly regions: Pressure histories of rod 2C

In the PWR-2 region the poisoned rod 2C does not experience any failure during the 200 seconds transient like the other rods containing burnable poisons.

The rupture zone for all three PWR sub-assembly regions is across four nodes (nodes 29÷32). This may support the theory [1] that the tendency for non-coplanar deformation to occur is attributed to the cooling of neighbouring rods resulting from perturbations in the flow field. If one rod deforms more rapidly than its neighbours, the coolant flow around it is reduced and the diverted flow enters neighbouring sub-channels, cooling surrounding rods more. The difference of pin power and internal pressure causes some rods to deform more rapidly, and thereby causes a wider rupture zone.

#### 3.4 Burst strains

The burst strain range for all three sub-assembly regions varies from 30% to 65% with an average burst strain of about 40%.

The presence of burnable poisons (Gadolinium) decreases both the internal gas pressure and the pin decay power, reducing the swelling. In any of the three PWR sub-assembly regions, none of the rods with burnable poisons (rod 4C in PWR-1 Case, rods 4C and 2C in PWR-2 Case and rod 5B in PWR-3 Case) do burst during the 200 seconds of the transient. The effect of burnable poisons in one rod is also passed on its surrounding rods. The enhanced cooling conditions around poisoned rods is observed to induce higher azimuthal temperature gradients in the adjacent rods leading to their lower strain failure. As example, the burst strain of rod 3D drops from 64% and 68% in PWR-1 and PWR-3 Cases to 51% in PWR-2 Case, where rod 2C is modelled to contain burnable poisons. An analogous response can be recognised for rod 4B in PWR-3 Case.

The burst strains calculated in the three regions are generally lower than MT-3 experimental data (particularly for rod 5C and 5D). This can be attributed to the augmented distinction among rods induced by different pin powers and initial gas pressures.

# 3.5 Blockage

The total blockage in the highest deformed section (from node 29 to node 32) for each of three sub-assembly regions is shown in Table 3.

The calculation of flow area reduction across the highest strain zone shows a blockage between 31% and 52% over about 120 mm. The highest axial blockage is observed in node 31, while the highest absolute blockage of 51.8 % is predicted in region PWR-1. Several experiments (ACHILLES [12], THETIS[13], FEBA[14]) have demonstrated that similar levels of blockage do not impair the cooling of the upper regions of the fuel assembly.

Node	PWR-1	PWR-2	PWR-3
29	40.85	39.58	39.7
30	45.90	45.22	42.97
31	51.80	49.93	48.75
32	34.04	31.04	35.72

Table 3 Flow Area Blockage

The predicted pin deformations of the three PWR sub-assembly regions in correspondence of the highest predicted assembly blockage (node 31; 2667.3÷2698.8 mm) have been combined together and opportunely replicated to reproduce the hypothetical blockage of the entire fuel assembly (Figure 11). The control rod guide thimbles are easily recognisable. The outer ring of rods in the assembly is assumed to undergo no deformation.

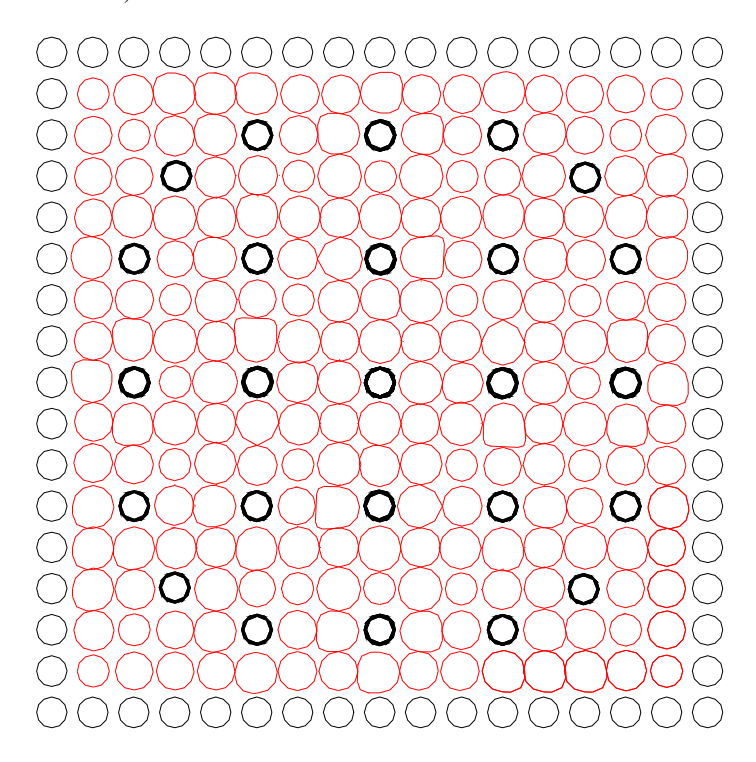


Figure 11 Fuel assembly blockage

# 4. Conclusions

The MATARE code has been used to analyse three different sub-assembly areas of a typical PWR fuel assembly during the reflood phase of a Loss-Of-Coolant Accident.

The temperature histories showed that rods containing burnable poisons experienced lower cladding temperatures due to the lower decay power while the other rods underwent the prolonged residence in the ductile temperature range of the upper zone of the  $\alpha$ -phase. However, neither long balloons nor large diametrical strains were observed in the sub-assembly regions.

The burst strain range for all three sub-assembly regions varies from 30% to 65% with an average burst strain of about 40%. The impact of burnable poisons on rod deformation is relevant, since no *poisoned* rod experienced failure during the 200 seconds of the transient. The presence of rods with burnable poisons also affects the behaviour of the adjacent rods. The enhanced cooling conditions that develop around the rods containing burnable poisons seem to increase the azimuthal temperature gradients of the neighbour rods leading to a lower burst strain.

The axial strain profile of the rods without burnable poisons shows the three typical ballooning peaks, already observed in the MT-3 experiment. The enhancement in heat transfer generated by the grids and reproduced by the MATARE grid-model, leads to *carrot*-shaped balloons with the region of significant growth restricted to the top end of each grid span.

The axial strain profile of the rods with burnable poisons is instead characterised by a plateau upstream the fifth grid and a peak at the upper elevation of the rods. The plateau is probably caused by the enhancement in cooling conditions that stops the swelling of the rod at that location. Better cooling conditions are due to the flow diversion because the *poisoned* rod swells less than the surrounding rods at the same axial location. Gd-poisoning of selected rods is, therefore, beneficial in further reducing the

clad ballooning problem. The only peak, though modest, is then at the upper elevation of the rod, where the cladding temperature is high enough to cause deformation.

The analysis of the azimuthal shape of the rods shows that the blockage in the sub-channels around guide thimbles and poisoned rods is low. This is probably caused by the flow diversion towards these elements, which provides high azimuthal temperature gradients in the surrounding rods such that failure occurs before serious blockage can take place.

The calculation of flow area reduction across the highest strain zone showed a blockage between 31% and 52% over about 120 mm. Several experiments (ACHILLES, THETIS, FEBA) have demonstrated that similar levels of blockage do not impair the cooling of the upper regions of the fuel assembly.

In conclusion, this application of MATARE has demonstrated the capability of the code to simulate the deformation of wide regions of a fuel assembly under reflood conditions and has shown how differences in pin pressure and power also contribute to a substantial incoherent ballooning.

# 5. References

- [1] Mann, C. A., Hindle, E. D., & Parsons, P. D., "The Deformation of PWR fuel in a LOCA." Rep. No. ND-R-701(S), 1982. UKAEA Northern Division.
- [2] Gibson, I.H., Coddington, P., Healey, T., Mann, C.A., "The UK MT-3 Ballooning Test in the Battelle NRU Loop." AEEW-R-1506, 1982. UKAEA Winfrith.
- [3] Ammirabile, L., Walker, S.P., "Analysis of the MT-3 clad ballooning reflood test using the multi-rod coupled MATARE code." Nuclear Engineering and Design 240, 2010, 1121-1131.
- [4] Ransom, W. H., "RELAP5/MOD3 Code manual. Volume I: Code Structure, System Models and Solution Methods.", 1997. INEL.
- [5] Bowring, R.H., "MABEL-2: A code to analyse cladding deformation in a loss-of-coolant accident. Part 1: General Description.", 1982. Reactor Systems Analysis Division, AEE, Winfrith: Dorchester.
- [6] Page R., "Description of the TALINK (Rev 1.4) code for the linkage of codes executing in parallel.", 1999. NNC Limited.
- [7] Ammirabile, L., "Coupled Mechanical Thermohydraulic Multi-pin Deformation Analysis of a PWR Poss of Coolant Accident.", 2003. PhD Thesis. Imperial College London.
- [8] Ammirabile, L., Walker, S.P., "Multi-pin modelling of PWR fuel pin ballooning during post-LOCA reflood." Nuclear Engineering and Design 238, 2008, 1448-1458.
- [9] Haste, T. J., "A study using the MABEL-2C code of the effects of pellet and cladding asymmetries on PWR fuel rod deformation under conditions relevant to the NRU MT-3 ballooning experiment.", 1983 (Rep. No. ND-R-876(S)). UKAEA.
- [10] Haste, T. J., "Modelling of the Effect of ifferent Mechanical Restraints on PWR Fuel Rod Deformation under Conditions Relevant to the NRU MT-3 Experiment using the MABEL-2D Code.", 1984 (Rep. No. ND-R-988(S)). UKAEA Northern Division Report.
- [11] Yao, S. C., Hochreiter, L. E., & Leech, W. J. "Heat-Transfer Augmentation in Rod Bundles Near Grid Spacers.", 1982. Journal of Heat Transfer 104, 76-81.

The 14<sup>th</sup> International Topical Meeting on Nuclear Reactor Thermalhydraulics, NURETH-14 Toronto, Ontario, Canada, September 25-30, 2011

- [12] Pearson, K. G. & Dore, P., "ACHILLES ballooned Cluster Experiments.", 1991. (Rep. No. AEEW-R 2590). UKAEA Winfrith.
- [13] Jowitt, D., Cooper, C. A. and Pearson, K. G., "The THETIS 80% blocked cluster experiment.", 1984. (Rep. No. AEEW-R 1767). AEE Winfrith.
- [14] Ihle, P. and Rust, K., "FEBA Flooding Experiments with Blocked Arrays Evaluation Report.", 1984 (Rep. No. KfK 3657).